J Mol Model (2008) 14:1083–1086
DOI 10.1007/s00894-008-0351-7

ORIGINAL PAPER

ONIOM DFT/PM3 calculation on the interaction between STI-571 and abelson tyrosine kinase

Yuan-Zhen Xiong · Pei-Yu Chen

Received: 20 May 2008 / Accepted: 7 July 2008 / Published online: 29 July 2008
© Springer-Verlag 2008

Abstract The ONIOM2 (B3LYP/6–31G (d, p): PM3) and B3LYP/6–31G (d, p) methods were applied to investigate the interaction between **STI-571** and abelson tyrosine kinase binding site. The complex of *N*-[4-methyl-3-(4-pyridin-3-yl-pyrimidin-2-ylamino)- phenyl]-benzamide (part of **STI-571**) and related 16 amino acid residues were found at B3LYP/6–31G (d, p) level to have hydrogen bonds and π....π stacking interaction, their binding energy via HAF optimization was −20.4 kcal mol^{-1}. The results derived from this study agreed well with the reported observation.

Keywords Abelson tyrosine kinase · Interaction · ONIOM2 · **STI571**

Introduction

Protein tyrosine kinases catalyse the transfer of the *r*-phosphory group of adenosine triphosphate (ATP) to tyrosine residue of substrate proteins, which correlate with the emergence and progression of numerous disease including cancer, diabetes, atherosclerosis and psoriasis [1, 2]. Among the kinases, of a fusion *Bcr* and tyrosine Kinase Abelson (*Abl*) gene encoding for aberrant tyrosine kinase activity contributes to the development of chronic myelogenous leukemia (CML). CML is a clonal hematopoietic stem cell disorder characterized by the presence of the philadelphia chromosome. Consequently, inhibition of *Abl* protein tyrosine kinase can suppress proliferation of its positive clones. The most potent inhibitor of *Abl* is **STI-571** (Fig. 1 (1)); a compound of 2-phenylaminopyrimidine series, has been identified to have exceptionally high affinity and high specificity for *Abl* kinase. It is currently admitted as a drug in CML by FDA [3, 4].

Despite several investigations on the inhibiting mechanism of **STI-571** have been reported [1–5], the detailed interaction based on theoretical study has not been reported. Better understanding in quantum chemistry is beneficial for further analysis of activities and for the design of inhibitors as pharmaceutical lead compounds. However, it is a challenge for theoreticians to treat accurately such a large molecular system. Recently, accurate molecular modeling for larger molecules, such as those in molecular biology, became feasible due to new developments in computational chemistry. For instance, the ONIOM (our own *n*-layered integrated molecular orbital and molecular mechanics) method has been introduced, its efficiency has been improved over the years [6]. In the ONIOM2 approach, the system is divided into two layers, a small part of which, such as the inhibitor and the reacting amino acids in the binding site of an enzyme, is treated at a high quantum chemical level, whereas the large surrounding region is modeled using a lower level of calculations.

P.-Y. Chen
Experiment center of Chemistry 330010,
Nanchang University,
Nanchang, People's Republic of China

Y.-Z. Xiong (✉)
Department of pharmacy 330006,
Nanchang University,
Nanchang, People's Republic of China
e-mail: 051103107@fudan.edu.cn

Y.-Z. Xiong
School of Pharmacy, 200031, Fudan University,
Shanghai, People's Republic of China

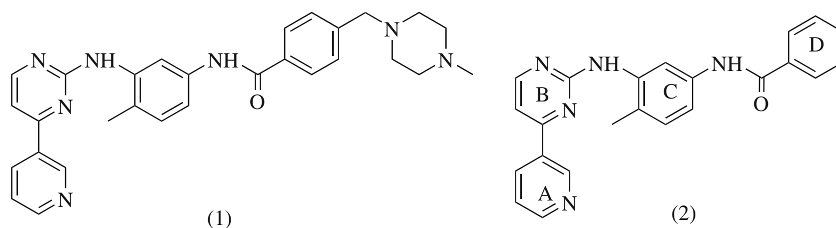

Fig. 1 **STI-571** (1) and ligand (2)

In the present study, we perform two-layer ONIOM calculations to simulate the interaction between **STI-571** and the amino acid residues in *abl* binding site. The model employed for the computation is the *Abl*-ligand X-ray structure (PDB code: 1FPU) [1]. Nevertheless, the ligand in the crystal structure is the pharmacophore of STI-571, whose name is *N*-[4-methyl-3-(4-pyridin-3-yl-pyrimidin-2-ylamino)-phenyl]-benzamide, it is composed by four rings (A, B, C, D), as indicated in Fig. 1 (2). This compound differs from **STI-571** in that it lacks piperazinyl attached to the phenyl-ring (ring D). In view of the fact that the piperazinyl is only likely to increase the solubility of the parent compound [1], we adopt this pharmacophore to represent **STI-571** and call it ligand in the whole paper. Thus, based on the X-ray structure, ONIOM2 (B3LYP/6–31G (d, p): PM3) and B3LYP/6–31G (d, p) methods are applied to carry out the study.

Computational section

The computational model contained those residues surrounding the binding site within the inner atomic distance of 6Å centered at the ligand. Related 16 amino acid residues were Glu286, Thr315, Tyr253, Phe382, Asn322, Gly321, Lue248, Leu370, Ala 269, Ile313, Lys271, Met290, Asp381, Val256, Met318 and Phe317, as shown in Fig. 2. All amino acids were assumed to be in their neutral forms, if not connected to another acid in the selected model, then H was added at N- and C- terminal with its bond, torsion

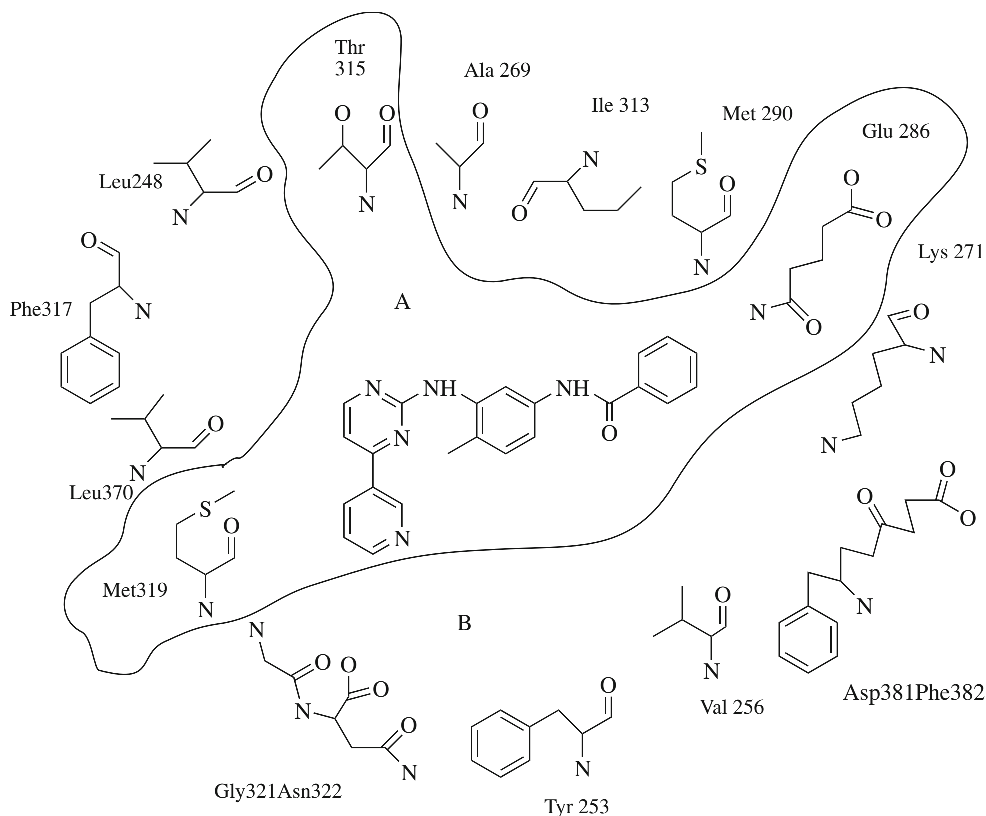

Fig. 2 The studied model system of ligand bound to *Abl* binding site. Layer partition for ONIOM2 (**a**) is the inner layer and (**b**) is the outer layer

angel was assumed to be the same as the X-ray structure. Thus, the “real” system in the present calculation consisted of 16 amino acid residues and the ligand, which contained 384 atoms.

The system was divided into two parts prior to optimization. According to the computational results of binding energies of the crystallographic structure at B3LYP/6–31G (d, p) level, the ligand and three reacting amino acid residues (Glu286,Thr 315 and Met 318) were treated at a high quantum chemical level. On the other hand, the large surrounding region (Tyr253, Phe382, Asn322, Gly321, Lue248, Leu370, Ala269, Ile313, Lys271, Met290, Asp381, Val 256, and Phe317) was coped with a lower layer of calculations (Fig. 2). Optimization was carried out via heavy atoms fixing (HAF) approximation. Amino acid residues/ pharmacophore system was depicted as the host-ligand complex. All the calculations were performed with the Gaussian 03 series of program. The optimized structures were visualized by Viewlite and Chem3D [7]. The ONIOM2 (B3LYP/6–31G (d, p):PM3) and B3LYP/6–31G (d, p) methods were applied to investigate the interaction between ligand and the 16 amino acid residues [8].

Energies of binding ($\Delta E_{\text{binding}}$) of the ONIOM2 calculations of the present system were calculated using the following formula:

$$\begin{aligned}&\Delta E_{\text{binding}}[\text{B3LYP}/6-31\text{G}(\text{d},\text{p}):\text{PM3}](\text{host}/\text{ligand})\\&=E[\text{B3LYP}/6-31\text{G}(\text{d},\text{p}):\text{PM3}](\text{host}/\text{ligand})\\&-E[\text{B3LYP}/6-31\text{G}(\text{d},\text{p}):\text{PM3}](\text{host})\\&-E[\text{B3LYP}/6-31\text{G}(\text{d},\text{p}):\text{PM3}](\text{ligand})\end{aligned}$$

Results and discussion

Table 1 lists the binding energies of inhibitor with individual residue surrounding the binding site at the B3LYP/6–31G (d, p) level of calculation. It can be seen that there are a number of Van der Waals interactions between the ligand and the amino acid residues, especially Val256 ($\Delta E=-2.7$ kcal mol^{-1}), Glu286 ($\Delta E=-2.2$ kcal mol^{-1}), Met290 ($\Delta E=-1.5$ kcal mol^{-1}) and Leu370 ($\Delta E=-1.0$ kcal mol^{-1}).

Figure 3 (a and b) show that the ligand also interact with the *Abl* kinase through hydrogen bonds. The hydroxyl hydrogen of Thr315 donates a H to the backbone O of the carbonyl amide of ligand (Fig. 3 (a)). The distance of this hydrogen bond is 1.94 Å for O-H...O=C, while in the crystal, it is 2.27 Å. The second hydrogen bond is between Met 318 and the ligand, the pyridinyl ring attached to the

Table 1 Binding energies of ligand with individual amino acid residue (kcal mol^{-1})

Amino acid	$\Delta E_{\text{binding}}$	Amino acid	$\Delta E_{\text{binding}}$	ΔE_{total}
Leu248	−0.02	Phe317	−0.7	
Ile 13	−0.6	Thr315	−4.1	
Val256	−2.7	Asp381Phe382	−3.4	
Ala269	−0.4	Met 318	−1.7	
Leu370	−1.0	Glu286	−2.2	
Lys271	−0.2	Met290	−1.5	
Tyr253	−1.0	Gly321Asn322	−1.0	
				−20.4

pyrimidine moiety accepts a H from the amide of Met318 (Fig. 3 (b)). This H is normally hydrogen bonded to the nitrogen N1 in ATP. The distance of the hydrogen bond (NH....N) on B3LYP/6–31G (d, p) is 2.95 Å, as in the crystal, it is 3.00 Å.

The aromatic rings of the inhibitor provide sufficient flexibility and exceptional level of surface, which allow favorable π-π interaction with amino acid residues Phe317, Tyr253 and Phe382. As shown in Fig. 3 (c–e), the pyridinyl ring (ring A) of the ligand is in parallel stacking configuration with the phenyl ring of Phe317 (Fig. 3 (c)), while the parallelism of the pyrimidin moiety (ring B) in the ligand and phenol ring in Tyr253 seem to form π....π stacking interaction (Fig. 3 (d)). The phenyl ring in Phe382 inserts into the phenyl ring (ring C) of the ligand, they make H....π and π....π (Fig. 3 (e)) interactions.

The obtained binding energies are −20.4 kcal mol^{-1} for the model at ONIOM2 (B3LYP/6–31G (d, p): PM3) and B3LYP/6–31G (d, p) methods, which indicates strong interaction in stabilizing the complex. Analyzing the composing of ONIOM2 binding energies, we find that the binding energy between Thr315 and the ligand is −4.1 kcal mol^{-1}, thus Thr315 accounts for facial interaction in the complex system [1].

Conclusions

ONIOM2 calculation of the complex show that they have strong interaction and the calculated binding energy is −20.4 kcal mol^{-1}. These interactions contain hydrogen bond, π....π stacking and van der Waals interaction, which is in accordance with the previous report [1]. The computational results demonstrate that the carbonyl of amide, ring A, B and C is necessary for the inhibition; structural modification may occur on ring D [9].

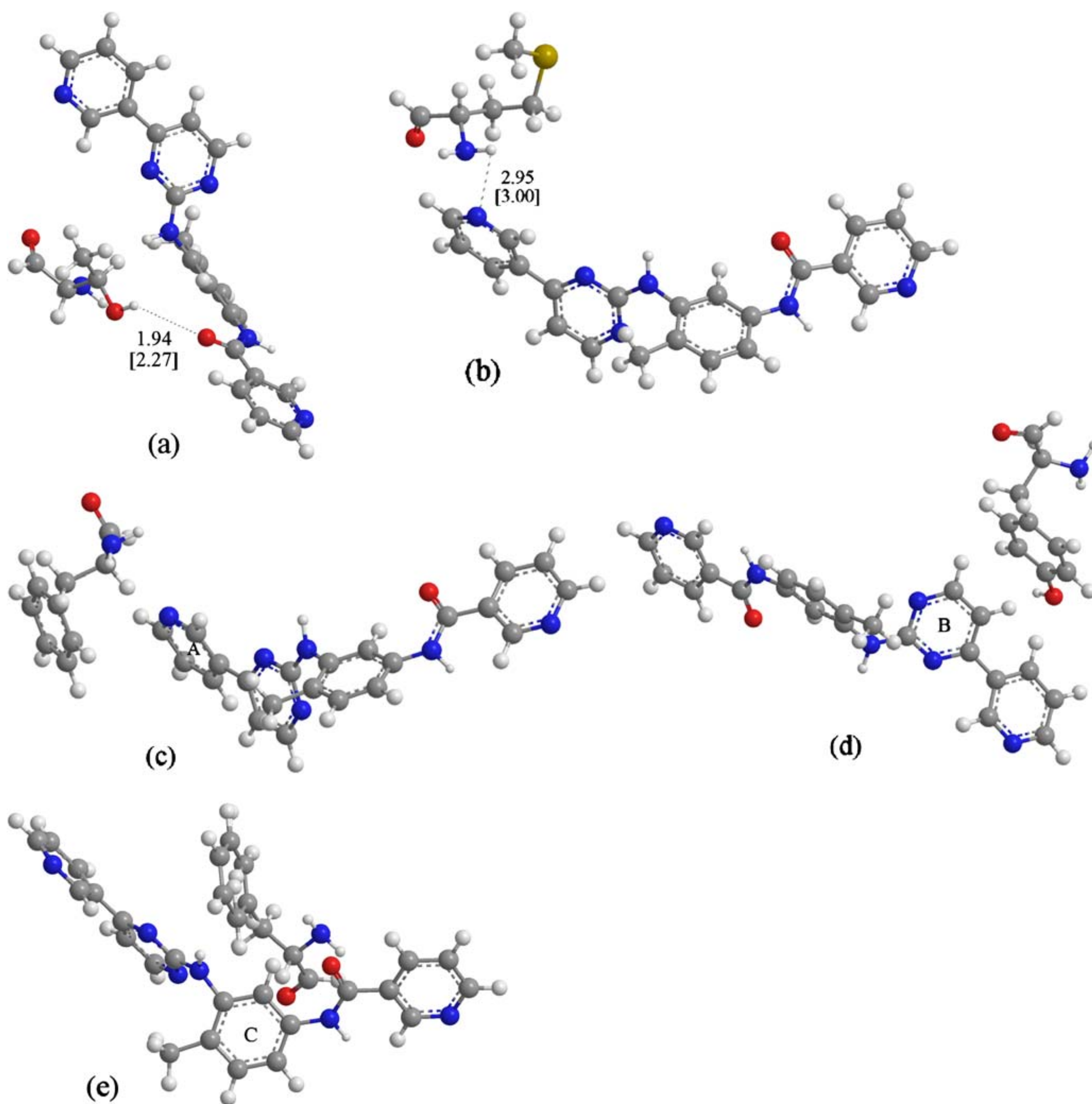

Fig. 3 Optimized structure of the ligand and individual amino acid residues (**a**) Thr 315, (**b**) Met 318, (**c**) Phe 317, (**d**) Tyr 253, (**e**) Phe382, complex from ONIOM(B3LYP/6–31G(d, p): PM3)

References

1. Schindler T, Bornmann W, Pellicena P, Miller WT, Clarkson B, Kuriyan J (2000) Sci 289(5486):1938–1942
2. Fernandez A, Maddipati A (2006) J Med Chem 49:3092–3100
3. Wolber G, Langer T (2005) J Chem Inf Model 45:160–169
4. Martin SE, Peterson BR (2002) J Peptide Sci 8:227–233
5. Szakacs Z, Beni S, Varga Z, Orfi L, Noszal B (2005) J Med Chem 48:249–255
6. Dapprich S, Komaromi I, Byun KS, Morokuma K, Frisch MJ (1999) J Mol Struct (Theochem) 461–462:1–21
7. Maseras F, Morokuma K (1995) J Comp Chem 16:1170–1179
8. Aronov AM, Baker C, Bemis GW (2007) J Med Chem 50:1280–1287
9. Das J, Chen P, Lin D, Padmanabha R, Lin J, Moquin RV, Shen ZQ, Cook LS, Doweyko AM, Pang SH, Shen DR, Qiong F, Fex HF, McIntyre KW, Shuster DJ, Gillooly KM, Behnia K, Schieven GL, Wityak J, Barrish JC (2006) J Med Chem 49:6819–6832